Kinetics of Conversion of $[Ir_4(CO)_{11}(PPh_2AuPPh_3)]$ into $[Ir_4(CO)_{10}(\mu\text{-}PPh_2)(\mu\text{-}AuPPh_3)]$ and their Structural Characterization†

Fatima S. Livotto,[a] Maria D. Vargas,*[,a] Dario Braga[b] and Fabrizia Grepioni[b]

[a] *Instituto de Quimica, Universidade Estadual de Campinas, CP 6154, Campinas, 13081, SP, Brazil*

[b] *Dipartimento di Chimica 'G. Ciamician', Universitá degli Studi di Bologna, Via F. Selmi 2, 40126 Bologna, Italy*

Deprotonation of $[Ir_4(CO)_{11}(PPh_2H)]$ **1** in the presence of $[Au(PPh_3)]PF_6$ yields the novel species $[Ir_4(CO)_{11}(PPh_2AuPPh_3)]$ **2** which possesses a tetrahedral framework bearing a terminally bonded PPh_2AuPPh_3 ligand. Changing the order of addition of the reagents results in the formation of $[Ir_4(CO)_{10}(\mu\text{-}PPh_2)(\mu\text{-}AuPPh_3)]$ **4** with bridging phosphido and $Au(PPh_3)^+$ units. Reaction of **4** with PPh_3 yields $[Ir_4(CO)_9(PPh_3)(\mu\text{-}PPh_2)(\mu\text{-}AuPPh_3)]$ **6**, while with the more basic phosphine $P(C_6H_4OMe\text{-}4)_3$ substitution of the PPh_3 at the $Au(PPh_3)^+$ unit occurs producing $[Ir_4(CO)_{10}(\mu\text{-}PPh_2)\{\mu\text{-}AuP(C_6H_4OMe\text{-}4)_3\}]$. Deprotonation of $[Ir_4(CO)_{10}(PPh_3)(PPh_2H)]$ in the presence of $[Au(PPh_3)]PF_6$ yields $[Ir_4(CO)_{10}(PPh_3)(PPh_2AuPPh_3)]$, which undergoes rearrangement to **6**. The kinetics of decarbonylation of compound **2** to give **4** has been investigated and a dissociative mechanism is suggested, confirmed by the activation parameters $\Delta H^{\ddagger} = 135.6 \pm 3.8$ kJ mol^{-1} and $\Delta S^{\ddagger} = 81.2 \pm 10.9$ J K^{-1} mol^{-1}.

Clusters containing the $Au(PR_3)^+$ fragment have been increasingly investigated.[1,2] The reason for this interest is related to the variety of co-ordination modes that the $Au(PR_3)^+$ unit can exhibit, and also to the isolobal analogy between this fragment and H^+.[1-5] The large majority of carbonyl cluster compounds reported contain the $Au(PR_3)^+$ unit linked directly to the metal framework, and especially when only one $Au(PR_3)^+$ group is present it usually occupies the same position as the H in analogous hydrido species.[6] There are only a few examples of replacement of a hydrogen by the $Au(PR_3)^+$ fragment bound to main-group elements or to main group-containing ligands linked to carbonyl clusters, *viz.* $[Fe_4H(CO)_{12}(CAuPPh_3)]$ and $[Fe_4H(CO)_{12}(CH)]$[7,8] which are isostructural and $[Ru_4H(CO)_{12}\{Au_2(PPh_3)_2\}B]$[9] and $[Fe_4(CO)_{12}\{Au_2(PPh_3)_2\}(BH)]$[10] which do not obey the isolobal analogy. The compound $[AuMn(CO)_3(\mu\text{-}PPh_2)(bipy)(PR_3)]PF_6$ (bipy = 2,2′-bipyridine) represents the only example of a $Au(PR_3)^+$ fragment being linked to a phosphido phosphorus.[11]

We now report the synthesis of $[Ir_4(CO)_{11}(PPh_2AuPPh_3)]$ **2** containing $Au(PR_3)^+$ in place of hydrogen in $[Ir_4(CO)_{11}(PPh_2H)]$ **1**.[12,13] Compound **2** readily loses a carbonyl and undergoes rearrangement to yield $[Ir_4(CO)_{10}(\mu\text{-}PPh_2)(\mu\text{-}AuPPh_3)]$ **4** which is isostructural with $[Ir_4H(CO)_{10}(\mu\text{-}PPh_2)]$ **5**.[14] Kinetic studies show that CO dissociation is the rate-determining step of the reaction. A brief communication of this work has been published.[15]

Results and Discussion

Preparation of $[Ir_4(CO)_{11}(PPh_2AuPPh_3)]$ **2** *and* $[Ir_4(CO)_{10}(\mu\text{-}PPh_2)(\mu\text{-}AuPPh_3)]$ **4**.—Deprotonation of yellow $[Ir_4(CO)_{11}(PPh_2H)]$ **1** with 1,8-diazabicyclo[5.4.0]undec-7-ene (dbu) in the presence of $[Au(PPh_3)]PF_6$ yielded the analogous compound $[Ir_4(CO)_{11}(PPh_2AuPPh_3)]$ **2** of the same colour. When the deprotonation reaction was performed in the absence of $[Au(PPh_3)]PF_6$, however, the anion $[Ir_4(CO)_{10}(\mu\text{-}PPh_2)]^-$ **3** first formed then reacted rapidly with $[Au(PPh_3)]PF_6$ to give the dark red compound $[Ir_4(CO)_{10}(\mu\text{-}PPh_2)(\mu\text{-}PPh_3)]$ **4**. Thus, the order of addition of the reagents was critical in the formation of these species, which were both obtained in yields above 90% and fully characterized by microanalyses and by spectroscopic measurements (Table 1 and 2).

The similarity between the IR spectra of compound **2** and $[Ir_4(CO)_{11}(PPh_3)]$[16] led us to formulate it as having the structure shown, in which the $Au(PPh_3)^+$ fragment bonds terminally to the PPh_2 phosphorus in place of the proton in **1** and with three bridging and eight terminal CO groups, instead of the all-terminal CO structure recently established for **1** in solution.[13] As has been thoroughly discussed previously,[17] steric effects would account for such structural differences. The $^{31}P\text{-}\{^1H\}$ NMR data are also in accord with this structure, as it exhibited two doublets at high field typical of phosphine phosphorus with a large J(P–P) 287.5 Hz (Table 2), indicating the proximity of the two P nuclei.

The $^{31}P\text{-}\{^1H\}$ NMR spectrum of compound **4** also showed the presence of two doublets, one at high field at δ 67.9, ^3J(P–P) 50.4 Hz (not 5 Hz as reported in ref. 15), due to the PPh_3 and the other one in the phosphide region at δ 229.7, slightly shifted from the values reported for the species $[Ir_4H(CO)_9L(\mu\text{-}PPh_2)]$, L = CO **5** and PPh_3 **5a** at δ 286.9 and 276.2, respectively.[14] In addition, the presence of a ν(CO) in the CO bridging region of the IR spectrum led us to formulate this compound as having the structure shown, with the $Au(PPh_3)$ group bridging the same metal–metal bond as the hydride in the analogous compound **5**.

Spectroscopic data for complexes **2** and **4** did not uniquely define their structures and hence single-crystal X-ray diffraction studies were undertaken.

Structures of Compounds **2** *and* **4**.—The molecular structures of compound **2** and **4** are closely related and will be described together. Relevant structural parameters for both species are listed in Tables 3 and 4. Views of compounds **2** and **4** are shown in Figs. 1 and 2 respectively, together with the atomic labelling.

† *Supplementary data available:* see Instructions for Authors, *J. Chem. Soc., Dalton Trans.*, 1992, Issue 1, pp. xx–xxv.

Table 1 Analytical[a] and physical data for the AuIr clusters

Compound	Colour	Yield[b] (%)	ν(CO)[c]/cm^{-1}	Analysis (%) C	H
2 $[Ir_4(CO)_{11}(PPh_2AuPPh_3)]$	Yellow	90	2082m, 2052vs, 2045vs, 2015m, 2003m, 1998m (sh), 1988w (sh), 1967vw (sh) 1880vw (sh), 1848m, 1832w, 1813m	28.5 (28.6)	1.40 (1.45)
4 $[Ir_4(CO)_{10}(\mu\text{-}PPh_2)(\mu\text{-}AuPPh_3)]$	Red	90	2070s, 2042vs, 2028vs, 2015vs, 2008s, 1995w, 1963w, 1838m	28.3 (28.4)	1.60 (1.50)
4a $[Ir_4(CO)_{10}(\mu\text{-}PPh_2)\{\mu\text{-}P(C_6H_4OMe\text{-}4)_3\}]$	Red	90	2070s, 2044vs, 2030vs, 2016vs, 2006s, 2001s (sh), 1978w, 1964w (br), 1827m (br)	29.0 (28.9)	1.90 (1.75)
6 $[Ir_4(CO)_9(PPh_3)(\mu\text{-}PPh_2)(\mu\text{-}AuPPh_3)]$	Red	90	2058s, 2020m, 2006vs, 1966w (br), 1804w, 1778vw	35.6 (35.5)	2.55 (2.05)
8 $[Ir_4(CO)_{10}(PPh_3)(PPh_2AuPPh_3)]$[d]	Orange	85	2058m, 2032s, 1998s (br), 1864vw, 1827w (br), 1795w (br)		

[a] Required values are given in parentheses. [b] Based on iridium. [c] In hexane, unless otherwise stated. [d] Undergoes easy conversion into **6**.

Table 2 Proton and $^{31}P\text{-}\{^1H\}$ NMR data for the AuIr clusters

Compound	$^{31}P\text{-}\{^1H\}$ NMR[a]
2	42.6 (d, PPh_3), 20.8 (d, PPh_2); J(P–P) = 287.5
4	229.7 (d, PPh_2), 67.9 (d, PPh_3); J(P–P) = 50.4
4a[b]	—
6	**A** 224.6 (dd, PPh_2), 68.9 (d, $AuPPh_3$), −1.8 (d, PPh_3);[c] ^3J(P–P) 50.2, ^2J(P–P) 14.7
	B 245.2 (br d, PPh_2), 69.1 (d, $AuPPh_3$), −1.8 (s, PPh_3);[c] ^3J(P–P) 50.3
	C 199.5 (d, PPh_2), 70.4 (d, $AuPPh_3$), 8.7 (s, PPh_3);[c] ^3J(P–P) 50.0
8	51.1 (d, $AuPPh_3$), 5.9 (d, PPh_2), −2.0 (s, PPh_3);[c] J(P–P) = 295.3

[a] In CD_2Cl_2 at room temperature unless otherwise specified; J in Hz. [b] ^1H NMR ($CDCl_3$): δ 3.83 (s, CH_3) and 7.00–7.51 (m, Ph). [c] In $CDCl_3$.

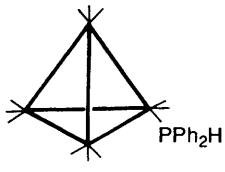

1

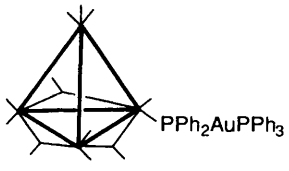

2

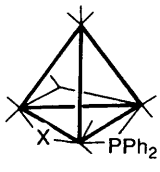

X

4 $AuPPh_3$

4a $AuP(C_6H_4OMe\text{-}4)_3$

5 H

Both species possess a tetrahedral iridium framework with Ir–Ir bond lengths ranging from 2.701(1) to 2.745(1) Å in **2** and from 2.689(2) to 2.832(2) Å in **4**. The ligand distribution recalls that observed in most Ir_4 derivatives, *i.e.* with the basal plane spanned by bridging ligands. These ligands are CO groups in **2**, while the basal plane in **4** bears one CO, the phosphide, and the $Au(PPh_3)$ groups. In **2** one terminal CO group is formally replaced by the PPh_2AuPPh_3 unit, which is linked to the cluster through the P atom of the PPh_2 fragment. It should be emphasized that this bonding mode is quite unusual in mixed-metal gold clusters. In most cases the $Au(PPh_3)$ fragment is found linked directly to the metal framework.

Table 3 Relevant bond distances (Å) and angles (°) for compound **2**

Ir(1)–Ir(2)	2.732(1)	Ir(4)–C(9)	1.91(3)
Ir(2)–Ir(3)	2.706(1)	Ir(4)–C(10)	1.84(3)
Ir(1)–Ir(3)	2.745(1)	Ir(4)–C(11)	1.88(3)
Ir(1)–Ir(4)	2.722(1)	P(1)–C(12)	1.84(2)
Ir(2)–Ir(4)	2.713(1)	P(1)–C(18)	1.85(2)
Ir(3)–Ir(4)	2.701(1)	P(2)–C(24)	1.76(2)
Ir(1)–P(1)	2.36(1)	P(2)–C(30)	1.82(3)
Au–P(1)	2.34(1)	P(2)–C(36)	1.80(2)
Au–P(2)	2.30(1)	C(1)–O(1)	1.15(3)
Ir(1)–C(1)	2.06(3)	C(2)–O(2)	1.15(3)
Ir(2)–C(1)	2.25(3)	C(3)–O(3)	1.15(3)
Ir(2)–C(2)	2.08(3)	C(4)–O(4)	1.15(3)
Ir(3)–C(2)	2.11(3)	C(5)–O(5)	1.13(2)
Ir(3)–C(3)	2.19(3)	C(6)–O(6)	1.14(2)
Ir(1)–C(3)	2.06(3)	C(7)–O(7)	1.08(3)
Ir(1)–C(4)	1.80(3)	C(8)–O(8)	1.14(3)
Ir(2)–C(5)	1.83(2)	C(9)–O(9)	1.08(3)
Ir(2)–C(6)	1.85(3)	C(10)–O(10)	1.19(3)
Ir(3)–C(7)	1.96(3)	C(11)–O(11)	1.12(3)
Ir(3)–C(8)	1.86(3)		
Ir(1)–P(1)–Au	113.4(2)	Au–P(2)–C(24)	116(1)
P(1)–Au–P(2)	177.9(2)	Au–P(2)–C(30)	109(1)
Ir(1)–P(1)–C(12)	111(1)	Au–P(2)–C(36)	115(1)
Ir(1)–P(1)–C(18)	113(1)		

Table 4 Relevant bond distances (Å) and angles (°) for compound **4**

Ir(1)–Ir(2)	2.778(2)	Ir(4)–C(8)	1.86(3)
Ir(2)–Ir(3)	2.832(2)	Ir(4)–C(9)	1.96(4)
Ir(1)–Ir(3)	2.736(2)	Ir(4)–C(10)	1.86(4)
Ir(1)–Ir(4)	2.689(2)	P(2)–C(11)	1.82(3)
Ir(2)–Ir(4)	2.739(2)	P(2)–C(17)	1.84(3)
Ir(3)–Ir(4)	2.719(2)	P(2)–C(23)	1.79(3)
Ir(1)–Au	2.788(2)	P(1)–C(29)	1.82(3)
Ir(3)–Au	2.731(2)	P(1)–C(35)	1.81(3)
Ir(2)–P(1)	2.36(1)	C(1)–O(1)	1.28(3)
Ir(3)–P(1)	2.29(1)	C(2)–O(2)	1.17(4)
Au–P(2)	2.27(1)	C(3)–O(3)	1.17(4)
Ir(1)–C(1)	2.01(3)	C(4)–O(4)	1.17(3)
Ir(2)–C(1)	2.01(3)	C(5)–O(5)	1.18(4)
Ir(1)–C(2)	1.83(5)	C(6)–O(6)	1.16(4)
Ir(1)–C(3)	1.86(4)	C(7)–O(7)	1.14(4)
Ir(2)–C(4)	1.90(3)	C(8)–O(8)	1.17(4)
Ir(2)–C(5)	1.83(4)	C(9)–O(9)	1.13(4)
Ir(3)–C(6)	1.82(4)	C(10)–O(10)	1.16(4)
Ir(3)–C(7)	1.87(4)		
Ir(1)–Au–Ir(3)	59.4(1)	Au–P(2)–C(11)	115(1)
Ir(2)–P(1)–Ir(3)	75.2(3)	Au–P(2)–C(17)	114(1)
C(29)–P(1)–C(35)	103(1)	Au–P(2)–C(23)	113(1)

The P–Au–P axis in compound **2** is strictly linear [177.9(2)°], and the Ir–P distance [2.36(1) Å] is comparable to those

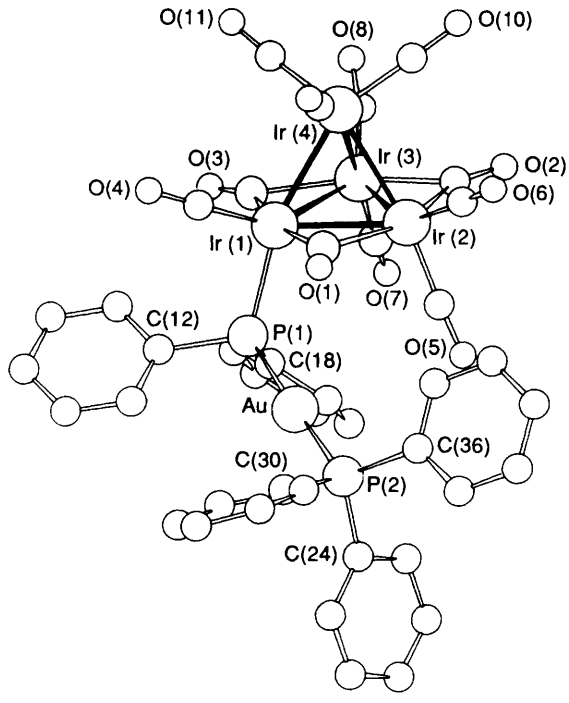

Fig. 1 Molecular structure of $[Ir_4(CO)_{11}(PPh_2AuPPh_3)]$ **2** showing the crystallographic numbering

observed in most phosphine-substituted Ir_4 species, implying that the dangling PPh_2AuPPh_3 ligand acts as a 'normal' monodentate phosphine. The Ir–P–Au bond angle of 113.4(2)° also indicates that the presence of the bulky $Au(PPh_3)$ fragment in place of a phenyl group on the phosphine does not cause appreciable intramolecular strain.

As almost invariably found in Ir_4 clusters containing bridging CO groups the Ir–Ir bonds spanned by the bridging ligands in compound **2** are longer [mean 2.728(1) Å] than the unbridged ones [mean 2.712(1) Å] confirming that the metal–metal bond 'shortening effect' usually attributed to the bridging CO groups in the M_4 derivatives is confined to the cobalt complexes.

The presence of more heterogeneous ligands over the framework of compound **4** is reflected in the wider range spanned by the Ir–Ir bond lengths (see above) and in a general swelling-up of the metal core with respect to **2** [mean Ir–Ir 2.720(1) in **2** *versus* 2.749(2) Å in **4**]. As expected, the three bridging ligands have quite different effects on the Ir–Ir bonds around the basal plane: while the Au-bridged bond is short [2.736(2) Å], the P-bridged one is the longest [2.832(2) Å], the CO-bridged bond being intermediate [2.778(2) Å]. Furthermore, there is an appreciable asymmetry of both Ir–P and Ir–Au bonding interactions [Ir(2)–P(1) 2.36(1), Ir(3)–P(1) 2.29(1), Ir(1)–Au 2.788(2), Ir(3)–Au 2.731(2) Å] both ligands being closer to the Ir atom in common.

The ligand distribution in compound **4** closely parallels that observed in $[Ir_4H(CO)_{10}(\mu\text{-}PPh_2)]$ **5**, which also contains a bridging phosphide group, while the place of the $AuPPh_3$ is 'taken' by the H (hydride) atom. This pair of Ir_4 clusters provides a nice example of the isolobal analogy between the H and $Au(PPh_3)$ ligands. The P-bridged bonds in this latter compound and in **4** have comparable lengths [2.796(2) *versus* 2.832(2) Å] as well as the H-bridged bond in **5** and the Au-bridged one in **4** [2.769(2) *versus* 2.736(2) Å].

Reactions of $[Ir_4(CO)_{10}(\mu\text{-}PPh_2)(\mu\text{-}AuPPh_3)]$ **4** *with Phosphines.*—Reaction of compound **4** with PPh_3 at 50 °C gives the monosubstituted compound $[Ir_4(CO)_9(PPh_3)(\mu\text{-}PPh_2)(\mu\text{-}AuPPh_3)]$ **6** in 60% yield. Carbonyl substitution in **4** needs more drastic conditions than those reported for the reactions of the analogous compound $[Ir_4(\mu\text{-}H)(CO)_{10}(\mu\text{-}PPh_2)]$ **5** with a series of phosphines and phosphites, which give $[Ir_4(\mu\text{-}H)(CO)_9L(\mu\text{-}PPh_2)]$.[14]

Kinetic studies of the reaction of compound **5** with PPh_3 have established an associative mechanism for the process.[18] If a similar mechanism is operative in the reaction of **4** with PPh_3, steric effects due to the presence of the $Au(PPh_3)^+$ unit would explain the relative reluctance of compound **4** to undergo nucleophilic attack at the metal centres. Significantly, the reaction of **4** with $P(C_6H_4OMe\text{-}4)_3$, a more basic phosphine than PPh_3, yields exclusively a product resulting from PPh_3 substitution on the Au atom, $[Ir_4(CO)_{10}(\mu\text{-}PPh_2)\{\mu\text{-}AuP(C_6H_4OMe\text{-}4)_3\}]$ **4a**, as shown by the ^1H NMR spectrum (Table 2).

Compound **6** was also produced from the thermolysis reaction of $[Ir_4(CO)_{10}(PPh_3)(PPh_2AuPPh_3)]$ **8** which was obtained by deprotonation of $[Ir_4(CO)_{10}(PPh_3)(PPh_2H]$ **7**[14] with dbu in the presence of $[Au(PPh_3)]PF_6$ as described for the synthesis of **2**. It was characterized on the basis of spectroscopic methods only, which indicated a structure similar to that of $[Ir_4(CO)_{10}(PPh_3)_2]$.[16,19]

The structure of $[Ir_4(\mu\text{-}H)(CO)_9(PPh_3)(\mu\text{-}PPh_2)]$ **5a** has been previously established in solution and in the solid state,[14] and shows that CO substitution with PPh_3 in **5** occurred in an axial position on a basal Ir atom,[12] not associated with the PPh_2 ligand.

Compound **6** has been characterized on the basis of spectroscopic and analytical data only (Tables 1 and 2), because X-ray-quality crystals could not be obtained. The IR spectrum exhibits ν_{CO} in the CO bridging region and the $^{31}P\text{-}\{^1H\}$ NMR spectrum shows the presence of three isomers in the

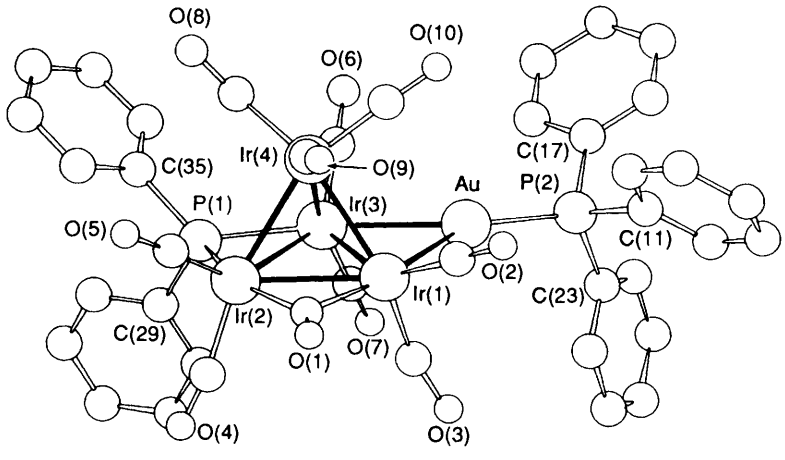

Fig. 2 Molecular structure of $[Ir_4(CO)_{10}(\mu\text{-}PPh_2)(\mu\text{-}AuPPh_3)]$ **4** showing the crystallographic numbering

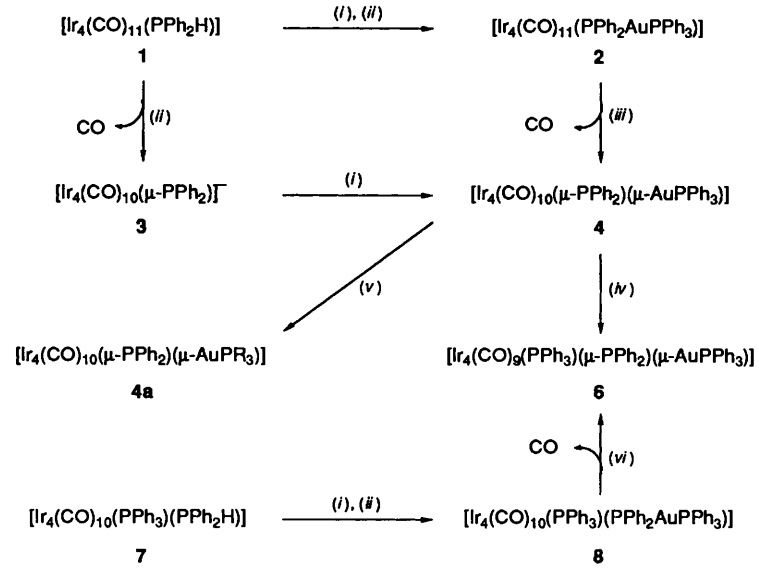

Scheme 1 Reagents and conditions: (*i*) 1.3 equivalents [Au(PPh$_3$)I] and 2 equivalents TlPF$_6$; (*ii*) 1.3 equivalents dbu; (*iii*) toluene, 80 °C, 30 min; (*iv*) 1 equivalent PPh$_3$, hexane, 50 °C, 3 h; (*v*) 1 equivalent P(C$_6$H$_4$OMe-4)$_3$, CH$_2$Cl$_2$; (*vi*) toluene, 70 °C, 15 min

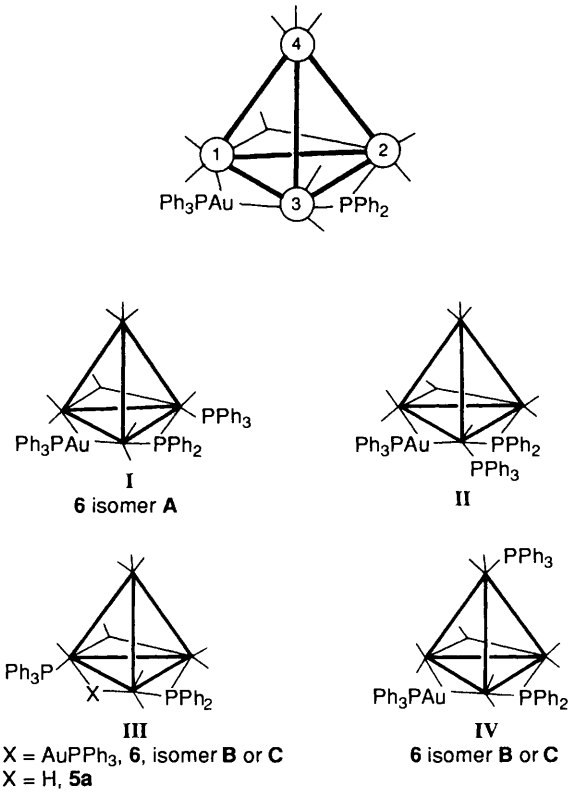

approximate ratio **A**:**B**:**C** = 6:15:0.3. In the three cases the presence of two strongly coupled resonances [^3J(P–P) ≈ 50 Hz], at high field due to the μ-PPh$_2$ phosphorus, and at low field attributed to the Au(PPh$_3$) phosphorus, suggests that the structures are similar to that of the unsubstituted species **4**, with the μ-PPh$_2$ and μ-Au(PPh$_3$) groups *trans* to each other, but with the PPh$_3$ ligand bound to different iridium atoms in each case.

The PPh$_3$ ligand in isomer **A** appears as a doublet at δ −1.8 coupled to the μ-PPh$_2$ phosphorus, ^2J(P–P) 14.7 Hz, and this isomer could therefore exhibit either structures **I** or **II** shown, with the PPh$_3$ bound to one of the iridium atoms linked to the μ-PPh$_2$ group, axially rather than radially for steric reasons. Owing also to steric hindrance at the Ir(3) atom, however, it seems reasonable to propose that structure **I** is more probable than structure **II** since there is much less crowding at this particular position.*

On the basis of the ^{31}P-{^{1}H} NMR data alone it is impossible to differentiate between isomers **B** and **C**, which can both exhibit either structure **III** or **IV**, as the PPh$_3$ phosphorus appears as a singlet at low field in each case. Structure **III** is similar to that established for the analogous compound **5a**, as shown, while structure **IV** represents the only other possible ligand distribution if one discards radial CO substitution on Ir(1) and Ir(2) for steric reasons.[16]

A comparison of the reactivities of the analogous compounds **4** and **5** indicates that substitution of H with Au(PPh$_3$) results in the end of site selectivity in the reactions with phosphines. Indeed, three of the four iridium centres, besides the Au atom (when a phosphine of higher basicity than PPh$_3$ is used) seem to become available to nucleophilic attack in **4**. Thus, the 'deactivation' of the Ir(1) position in **4**, which has been shown to undergo preferential CO substition in **5**, is most probably due to the steric bulk of the Au(PPh$_3$) moiety.

Rearrangement of Compounds **2** *and* **8** *into* **4** *and* **6**, *respectively*.—The positive ion fast atom bombardment (FAB) mass spectrum of compound **4** exhibited a molecular ion corresponding to [*M* + H]$^+$ and fragments due to sequential loss of seven CO ligands, a phenyl group and a PPh$_3$ ligand, as has been reported for the analogous compounds **5**, **5a** and [Ir$_4$(CO)$_{10}$(μ-PPh$_2$)(μ-AuPMe$_2$Ph)] **4b**.[20] In the case of compound **2**, however, the molecular ion detected corresponded to [*M* + H − CO]$^+$, and the fragmentation pattern was identical to that of compound **4**, which suggested that **2** was losing CO and rearranging to yield **4** during bombardment.

The FAB mass spectrum of compound **8** gave the molecular ion [*M* + H]$^+$, but also the molecular ion [*M* + H]$^+$ corresponding to **6**, thus indicating that a rearrangement of **8** to **6** was also occurring during bombardment. These results prompted us to investigate the thermal reactions of **2** and **8**, as a relationship has often been noted between processes observed in the FAB mass spectra and the solution chemistry of compounds under investigation.[20]

Quantitative conversion of compound **2** into **4** was observed upon heating at 70 °C for 2.5 h in toluene, as a result of loss of

* One of the referees has pointed out that the lack of coupling observed between the Au(PPh$_3$) unit and the PPh$_3$ also suggests that this isomer has structure **I** rather than **II**, although this is not conclusive.

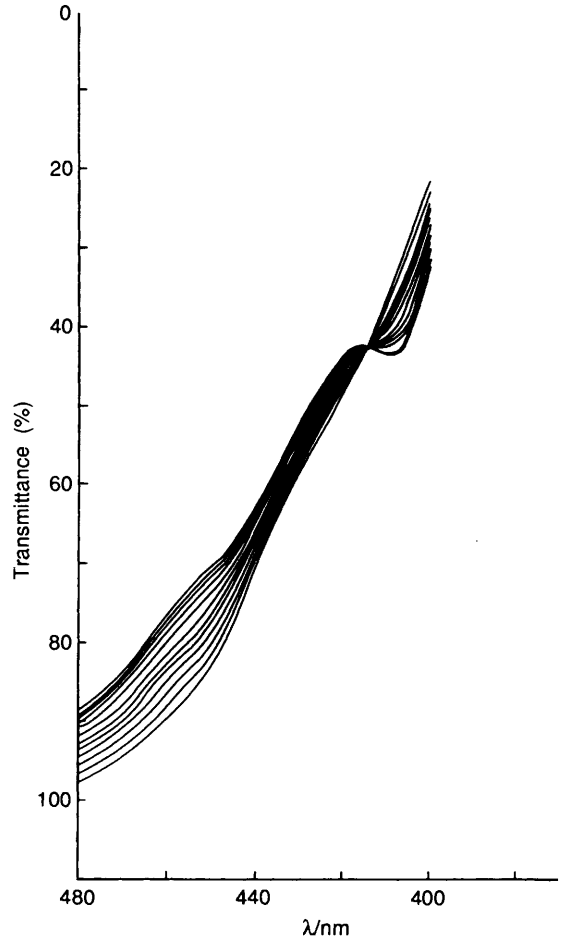

Fig. 3 Spectral changes upon thermolysis at 80 °C of a 8.0 × 10^{-5} mol dm^{-3} solution of $[Ir_4(CO)_{11}(PPh_2AuPPh_3)]$ **2** in toluene

Table 5 First-order rate constants for the conversion of $[Ir_4(CO)_{11}(PPh_2AuPPh_3)]$ **2** into $[Ir_4(CO)_{10}(\mu\text{-}PPh_2)(\mu\text{-}AuPPh_3)]$ **4**

T/°C	10^5[cluster]/ mol dm^{-3}	10^4k_1 [a]/s^{-1}	σ [b]
70.0	5.8	2.31	(1.1)
	8.0	3.00	
	10.0	2.88	
73.0	5.8	4.42	(0.73)
	8.0	3.89	
	10.0	3.81	
75.0	5.8	6.28	(0.54)
	8.0	5.85	
	10.0	6.01	
78.0	5.8	8.72	(0.36)
	8.0	8.02	
	10.0	7.94	
80.0	5.8	11.03	(1.38)
	8.0	11.10	
	10.0	10.96	

[a] The values of k_1 tabulated are the averages at each concentration. [b] Error limits are quoted as 95% confidence interval.

CO ligand and oxidative addition of the co-ordinated PPh_2Au-PPh_3 ligand in **2**, while conversion of **8** into **6** occurred upon heating at 70 °C for 15 min in toluene. The latter rearrangement was much faster, as expected, on the basis of previous kinetic results for the CO substitution reactions of $[Ir_4(CO)_{12-n}L_n]$, with L = PPh_3, $P(OPh)_3$ or PBu_3, where the rates have been found to increase with increasing substitution.[21]

Table 6 First-order constants and activation parameters for CO dissociation in $[Ir_4(CO)_{11}L]$ at 80 °C [23]

L	θ/°	Δh.n.p.[a] /mV	10^5k_1 /s^{-1}	$\Delta H^{\ddagger}$/kJ mol^{-1}	$\Delta S^{\ddagger}$/J K^{-1} mol^{-1}
$P(OPh)_3$ [b]	128	875	1	128.0 (3.3)	29.3 (9.6)
PPh_3 [b]	145	573	15	133.9 (4.2)	59.8 (11.3)
PBu_3 [b]	132	131	29	138.1 (1.7)	77.0 (4.6)
PPh_2AuPPh_3 [c]	145?	—	110	135.6 (3.8)	81.2 (10.9)

[a] Δh.n.p. = Difference in half-neutralization potential relative to *N,N'*-diphenylguanidine. The smaller its value, the greater the proton basicity. [b] In chlorobenzene. [c] In toluene.

Kinetics of Rearrangement of Compound **2** *to* **4**.—Measurements of the absorbance at time t, A_t, were made at 460 nm where the largest spectral differences between compounds **2** and **4** were observed (Fig. 3). The electronic spectra showed an isosbestic point at 414 nm, indicating that intermediates produced during the reaction were not formed in detectable concentration under these conditions.[22] The temperature range was 70–80 °C, since at lower temperatures the reaction was slow and decomposition occurred and at higher temperatures we had thermostatting problems.

Plots of ln A_t *versus* time were linear for a minimum of three half-lives. The k_{obs} values obtained were independent of the cluster concentration, suggesting a dissociative mechanism, with CO dissociation being the rate-determining path, according to $k_1 = k_{obs}$. The first-order rate constants obtained at different temperatures and ligand concentrations investigated are given in Table 5. The activation parameters $\Delta H^{\ddagger}$ = 135.6 ± 3.8 kJ mol^{-1} and $\Delta S^{\ddagger}$ = 81.2 ± 10.9 J K^{-1} mol^{-1} are consistent with a dissociative mechanism for this transformation and are comparable with those found for CO dissociation in the reactions of $[Ir_4(CO)_{11}L]$ with L' [L and L' = PR_3 or $P(OR)_3$], shown in Table 6 for comparison.[23]

The acceleration caused by CO substitution in $[Ir_4(CO)_{11}L]$ has been proposed to be electronic in nature since the rate increases with increasing electron-donor character of the P-donor substituents,[23] and therefore our activation parameters suggest that PPh_2AuPPh_3 is the most basic of the phosphines studied.

It has been reported[14] that compound **1** undergoes decarbonylation, oxidative addition of the P–H bond and formation of the analogous hydrido cluster **5** under more drastic conditions (toluene, 100 °C, 1.5 h), when compared with **2**. The major isomer of **1** in solution does not contain any bridging CO ligands and the structural change needed to produce **5** was most probably responsible for the slower rates of substitution.[21] The mechanism for this transformation would involve first CO dissociation to yield an unsaturated intermediate of the sort '$Ir_4(CO)_{10}(PPh_2AuPPh_3)$', and secondly oxidative addition of the P–Au bond to the metal core to yield **4**.

Although formation of phosphido and phosphinidene cluster compounds upon thermolysis of PPh_2H- and $PPhH_2$-containing clusters, respectively, is now a well established phenomenon,[24,25] conversion of **2** into **4** represents the first example of an oxidative addition of an Au–P bond to a cluster compound and provides another example of the isolobal analogy between the H and $Au(PPh_3)^+$ ligands.

Experimental

All manipulations and reactions were performed under an atmosphere of dry argon, unless otherwise specified, by using Schlenk-type glassware. Tetrahydrofuran (thf) was dried over sodium and benzophenone, dichloromethane over $LiAlH_4$, hexane over sodium and acetonitrile over phosphorus pentaoxide. All solvents were distilled under argon before use.

The progress of the reactions was monitored by infrared

Table 7 Crystal data and details of measurements for compounds **2** and **4**[a]

Formula	$C_{41}H_{25}Au_1Ir_4O_{11}P_2$	$C_{40}H_{25}Au_1Ir_4O_{10}P_2$
M_r	1721.3	1693.3
Crystal size (mm)	0.15 × 0.12 × 0.20	0.10 × 0.10 × 0.20
a/Å	9.336(6)	11.836(5)
b/Å	16.308(4)	27.581(5)
c/Å	28.862(7)	14.532(2)
β/°	93.06(3)	113.27(2)
U/Å^3	4387.8	4358.0
$F(000)$	3103	3048
D_c/g cm^{-3}	2.61	2.58
μ(Mo-Kα)/cm^{-1}	149.7	150.7
θ Range/°	2.0–20	2.0–25.0
ω scan width/°	0.6	0.8
Maximum scan time (s)	120	100
Measured reflections	4372	8145
Unique observed reflections [$I_o > 2\sigma(I_o)$]	2130	2576
Minimum, maximum absorption corrections	0.65, 1.10	0.84, 1.32
R, R', S	0.028, 0.027, 1.37	0.052, 0.046, 1.68
K, g	1.1, 0.0003	1.8, 0.0007

[a] Details in common: monoclinic, space group $P2_1/n$; $Z = 4$; requested counting $\sigma(I)/I = 0.01$; prescan rate 5 min^{-1}; prescan acceptance $\sigma(I)/I$ 0.5; octants explored $\pm h$, $+k$, $+l$. [b] $R' = \Sigma[(F_o - F_c)w^{\frac{1}{2}}]/\Sigma(F_o w^{\frac{1}{2}})$, where $w = k/[\sigma(F) + |g|F^2]$.

spectroscopy between 2200 and 1600 cm^{-1}, using CaF_2 cells 0.5 mm thick, recorded on a JASCO IR-700 spectrometer, or by analytical TLC (silica gel 60G Merck or Fluka). Preparative TLC was carried out in air by using *ca.* 1.0 mm thick glass-backed silica gel plates (20 × 20 mm) with silica gel 60G (Merck or Fluka). All substituted Ir_4 clusters were stored under an inert atmosphere, for they were found to be slightly air sensitive in the solid state.

Proton and ^{31}P NMR spectra were recorded on a Bruker 400 AM or a Varian XL100 instrument, using deuteriated solvents as lock, and as references $SiMe_4$ for ^1H and H_3PO_4 for ^{31}P. Fast atom bombardment mass spectra were obtained on a KRATOS MS 50 spectrometer, the atom beam being produced by an Ion Tech FAB gun operating with xenon at 8 kV and a current of 40 μA; *p*-nitrobenzyl alcohol was used as the matrix. All *m/z* values are referred to ^{193}Ir.

The compounds $[Ir_4(CO)_{12}]$[26] and $[Ir_4(CO)_{11}L]$ (L = PPh_2H[12,13] or PPh_3[16]) were prepared according to published procedures. 1,8-Diazabicyclo[5.4.0]undec-7-ene was distilled *in vacuo*. All the other reagents were purchased from commercial sources and used as supplied.

Preparation of $[Ir_4(CO)_{11}(PPh_2AuPPh_3)]$ **2**.—A grey suspension of $[Au(PPh_3)I]$ (18 mg, 0.031 mmol) and $TlPF_6$ (17 mg, 0.048 mmol) in CH_2Cl_2 (4 cm^3) was stirred for 1 h at room temperature (r.t.), after which time it turned yellow-green. After adding a yellow solution of $[Ir_4(CO)_{11}(PPh_2H)]$ **1** (30 mg, 0.024 mmol) in CH_2Cl_2 (8 cm^3) to the suspension, and stirring for 10 min, the mixture was treated with dbu (4.6 μl, 0.031 mmol) with no colour change. After 10 min of stirring the mixture was filtered through silica under argon, and the solvent was evaporated *in vacuo*. Purification by preparative TLC with CH_2Cl_2–hexane (1:1) afforded only $[Ir_4(CO)_{11}(PPh_2AuPPh_3)]$ **2** (37 mg, 90%).

Preparation of $[Ir_4(CO)_{10}(\mu\text{-}PPh_2)(\mu\text{-}AuPPh_3)]$ **4**.—A yellow solution of $[Ir_4(CO)_{11}(PPh_2H)]$ **1** (30 mg, 0.024 mmol) in CH_2Cl_2 (8 cm^3) was treated with dbu (4.6 μl, 0.031 mmol) at 25 °C, resulting in an immediate colour change. After 10 min of stirring, this mixture was added to a suspension of $[Au(PPh_3)I]$ (18 mg, 0.031 mmol) and $TlPF_6$ (17 mg, 0.048 mmol) in CH_2Cl_2 (4 cm^3), previously stirred for 1 h. The solution turned bright red. It was filtered through silica under argon and the solvent was evaporated *in vacuo*. After purification by preparative TLC with CH_2Cl_2–hexane (1:1) the only product obtained was $[Ir_4(CO)_{10}(\mu\text{-}PPh_2)(\mu\text{-}AuPPh_3)]$ **4** (37 mg, 90%). FAB mass spectrum: *m/z* 1967 $[M + H]^+$.

Reactions of Compound **4**.—*With* PPh_3. A solution containing PPh_3 (5 mg, 0.017 mmol) in hexane (2.5 cm^3) was added to a solution of compound **4** (30 mg, 0.017 mmol) in hexane (10 cm^3) and the mixture was left to stir at 50 °C for 2 h. The solvent was then evaporated, and the mixture purified by TLC with CH_2Cl_2–hexane (1:1), affording $[Ir_4(CO)_9(PPh_3)(\mu\text{-}PPh_2)(\mu\text{-}AuPPh_3)]$ **6** (20 mg, 60%) and an unidentified product, besides decomposition.

With $P(C_6H_4OMe\text{-}4)_3$. To a bright red solution of compound **4** (50 mg, 0.030 mmol) in CH_2Cl_2 (10 cm^3) was added dropwise a solution of $P(C_6H_4OMe\text{-}4)_3$ (11 mg, 0.030 mmol) in CH_2Cl_2 (3 cm^3). The reaction was monitored by analytical TLC with CH_2Cl_2–hexane (1:1), as changes neither in the colour nor in the IR spectrum of the mixture were observed. After 15 min of stirring the mixture was purified by preparative TLC (same eluent as above), affording $[Ir_4(CO)_{10}(\mu\text{-}PPh_2)\{\mu\text{-}AuP(C_6H_4OMe\text{-}4)_3\}]$ **4a** (47 mg, 90%).

Preparation of $[Ir_4(CO)_{10}(PPh_3)(PPh_2AuPPh_3)]$ **8**.—To a suspension of $TlPF_6$ (69 mg, 0.20 mmol) and $[Au(PPh_3)I]$ (70 mg, 0.12 mmol) in CH_2Cl_2 (8 cm^3) stirred for 1 h at r.t. was added a solution of $[Ir_4(CO)_{10}(PPh_3)(PPh_2H)]$ **7** (150 mg, 0.10 mmol) in CH_2Cl_2 (20 cm^3). After the mixture had been stirred for 10 min it was treated with dbu (17 μl, 0.12 mmol) and stirred for 10 min. It was then filtered under an inert atmosphere and the solvent evaporated *in vacuo*. Crystallization from hexane produced $[Ir_4(CO)_{10}(PPh_3)(PPh_2AuPPh_3)]$ **8** (0.166 mg, 85%). FAB mass spectrum: *m/z* 1959 $[M + H]^+$.

Rearrangement of Compound **8** *into* $[Ir_4(CO)_9(PPh_3)(\mu\text{-}PPh_2)(\mu\text{-}AuPPh_3)]$ **6**.—A solution of compound **8** (30 mg, 0.015 mmol) in toluene (10 cm^3) was heated at 70 °C for 15 min. After this time the solvent was evaporated and the mixture purified by preparative TLC with CH_2Cl_2–hexane (1:1) affording $[Ir_4(CO)_9(PPh_3)(\mu\text{-}PPh_2)(\mu\text{-}AuPPh_3)]$ **6** (26 mg, 90%). FAB mass spectrum: *m/z* 1931 $[M + H]^+$.

Kinetics of the Transformation of $[Ir_4(CO)_{11}(PPh_2AuPPh_3)]$ **2** *into* $[Ir_4(CO)_{10}(\mu\text{-}PPh_2)(\mu\text{-}AuPPh_3)]$ **4**.—The kinetics of the reaction was conveniently monitored with a Carl Zeiss DMR21 spectrophotometer over the wavelength range 500–400 nm. The stock solution was made in a Schlenk glass using toluene as a solvent, of concentration of 5.8×10^{-4} mol dm^{-3}. The stock solution was diluted in an UV/VIS cell in the concentration range 5.8×10^{-5}–10.0×10^{-5} mol dm^{-3}. Samples were placed in the thermostatted cell holder of the spectrophotometer (70.0–80.0 ± 0.1 °C) and left to attain thermal equilibrium. The k_{obs} values were calculated using the kinetic over-relaxation method (KORE)[27] and a SID 501 computer. The values of $\Delta H^\ddagger$ and $\Delta S^\ddagger$ were obtained by a non-weighted linear least-squares analysis of the dependence of the individual values of $\ln(k_1/T)$ on $1/T$. The uncertainties quoted are standard deviations corrected for the number of degrees of freedom, so that 95% confidence limits can be obtained by multiplying by the appropriate Student's factor (1.96) for an infinite number of degrees of freedom.

Structural Characterization of Compounds **2** *and* **4**.—Crystal data and details of measurements for compounds **2** and **4** are summarized in Table 7. Intensity data for both species were collected at room temperature on a Enraf-Nonius CAD4 diffractometer by the ω–2θ scan method, using Mo-Kα radiation (λ = 0.710 69 Å). Fast decay under X-ray exposure and poor diffraction of the crystal prevented extension of data collection

Table 8 Fractional atomic coordinates for compound **2**

Atom	*x*	*y*	*z*	Atom	*x*	*y*	*z*
Ir(1)	0.174 26(10)	0.155 75(6)	0.675 23(4)	C(13)	0.247 8(18)	−0.006 8(10)	0.586 6(4)
Ir(2)	−0.002 54(10)	0.256 48(6)	0.721 80(4)	C(14)	0.330 9(18)	−0.047 8(10)	0.555 3(4)
Ir(3)	0.071 28(11)	0.108 78(6)	0.758 50(4)	C(15)	0.309 9(18)	−0.032 9(10)	0.507 8(4)
Ir(4)	0.269 71(11)	0.229 00(6)	0.755 83(4)	C(16)	0.205 7(18)	0.023 1(10)	0.491 7(4)
Au	−0.104 06(11)	0.201 33(6)	0.571 54(4)	C(17)	0.122 5(18)	0.064 1(10)	0.523 1(4)
P(1)	0.032 5(7)	0.102 0(4)	0.612 1(2)	C(18)	−0.0911(13)	0.020 1(10)	0.629 4(5)
P(2)	−0.231 6(7)	0.302 2(4)	0.531 7(3)	C(19)	−0.050 5(13)	−0.060 8(10)	0.638 8(5)
C(1)	0.119 8(25)	0.274 5(16)	0.657 6(9)	C(20)	−0.152 4(13)	−0.117 7(10)	0.651 8(5)
O(1)	0.126 8(20)	0.327 4(12)	0.631 4(7)	C(21)	−0.294 9(13)	−0.093 8(10)	0.655 4(5)
C(2)	−0.054 2(27)	0.204 2(17)	0.784 4(10)	C(22)	−0.335 5(13)	−0.013 0(10)	0.645 9(5)
O(2)	−0.116 2(24)	0.215 6(10)	0.817 0(6)	C(23)	−0.233 6(13)	0.044 0(10)	0.632 9(5)
C(3)	0.202 4(23)	0.045 5(18)	0.709 1(8)	C(24)	−0.393 4(21)	0.271 8(11)	0.503 0(7)
O(3)	0.249 9(19)	−0.019 5(11)	0.706 4(7)	C(25)	−0.428 3(21)	0.271 8(11)	0.455 4(7)
C(4)	0.338 5(30)	0.154 6(18)	0.645 2(10)	C(26)	−0.565 0(21)	0.247 8(11)	0.438 8(7)
O(4)	0.446 4(21)	0.153 8(13)	0.627 8(8)	C(27)	−0.666 8(21)	0.223 9(11)	0.469 8(7)
C(5)	−0.185 4(25)	0.247 1(17)	0.695 8(9)	C(28)	−0.631 9(21)	0.223 9(11)	0.517 4(7)
O(5)	−0.299 7(20)	0.243 1(11)	0.681 3(7)	C(29)	−0.495 2(21)	0.247 9(11)	0.534 0(7)
C(6)	−0.011 1(24)	0.367 1(16)	0.735 1(9)	C(30)	−0.128 5(23)	0.338 3(10)	0.483 8(9)
O(6)	−0.011 2(20)	0.436 1(12)	0.741 3(8)	C(31)	−0.071 0(23)	0.279 5(10)	0.455 0(9)
C(7)	−0.092 4(30)	0.033 1(18)	0.752 4(10)	C(32)	−0.006 3(23)	0.303 6(10)	0.414 8(9)
O(7)	−0.181 2(21)	−0.008 0(13)	0.750 6(7)	C(33)	0.001 0(23)	0.386 6(10)	0.403 3(9)
C(8)	0.144 6(36)	0.058 2(17)	0.812 6(10)	C(34)	−0.056 5(23)	0.445 4(10)	0.432 1(9)
O(8)	0.216 4(26)	0.031 1(14)	0.841 9(8)	C(35)	−0.121 3(23)	0.421 2(10)	0.472 4(9)
C(9)	0.360 5(32)	0.316 1(17)	0.724 5(11)	C(36)	−0.278 8(21)	0.389 5(14)	0.565 7(6)
O(9)	0.413 0(22)	0.368 9(12)	0.710 2(8)	C(37)	−0.387 6(21)	0.443 2(14)	0.550 4(6)
C(10)	0.237 1(31)	0.271 4(21)	0.813 3(10)	C(38)	−0.422 8(21)	0.509 9(14)	0.577 8(6)
O(10)	0.219 6(24)	0.301 2(13)	0.850 0(7)	C(39)	−0.349 2(21)	0.523 0(14)	0.620 5(6)
C(11)	0.431 9(32)	0.161 6(16)	0.766 6(10)	C(40)	−0.240 4(21)	0.469 3(14)	0.635 8(6)
O(11)	0.527 6(22)	0.121 9(12)	0.774 7(8)	C(41)	−0.205 2(21)	0.402 5(14)	0.608 4(6)
C(12)	0.143 6(18)	0.049 2(10)	0.570 6(4)				

Table 9 Fractional atomic coordinates for compound **4**

Atom	*x*	*y*	*z*	Atom	*x*	*y*	*z*
Ir(1)	0.022 73(12)	0.125 79(5)	0.220 07(10)	C(13)	0.063 9(20)	0.097 7(6)	0.726 8(16)
Ir(2)	0.055 60(12)	0.134 43(5)	0.041 81(10)	C(14)	0.013 9(20)	0.144 0(6)	0.700 1(16)
Ir(3)	0.255 80(12)	0.116 64(5)	0.226 18(10)	C(15)	0.045 1(20)	0.172 0(6)	0.633 7(16)
Ir(4)	0.138 90(13)	0.203 77(5)	0.188 26(11)	C(16)	0.126 2(20)	0.153 8(6)	0.594 0(16)
Au	0.221 04(13)	0.106 98(5)	0.400 18(10)	C(17)	0.434 2(20)	0.106 6(9)	0.645 5(18)
P(1)	0.262 6(7)	0.118 5(3)	0.071 2(7)	C(18)	0.464 4(20)	0.122 1(9)	0.743 7(18)
P(2)	0.278 9(8)	0.086 1(3)	0.563 2(7)	C(19)	0.584 5(20)	0.136 4(9)	0.802 4(18)
C(1)	−0.092 0(27)	0.138 6(10)	0.077 5(21)	C(20)	0.674 4(20)	0.135 2(9)	0.762 9(18)
O(1)	−0.206 6(24)	0.146 9(10)	0.040 8(20)	C(21)	0.644 2(20)	0.119 7(9)	0.664 7(18)
C(2)	−0.061 6(37)	0.155 0(15)	0.286 9(31)	C(22)	0.524 2(20)	0.105 4(9)	0.606 0(18)
O(2)	−0.114 2(27)	0.171 9(11)	0.332 0(23)	C(23)	0.280 4(19)	0.021 8(10)	0.581 9(16)
C(3)	−0.005 5(34)	0.060 2(14)	0.233 3(29)	C(24)	0.179 1(19)	−0.005 1(10)	0.519 8(16)
O(3)	−0.032 3(25)	0.021 8(10)	0.252 8(20)	C(25)	0.177 1(19)	−0.055 2(10)	0.531 5(16)
C(4)	−0.012 2(24)	0.078 7(10)	−0.036 9(20)	C(26)	0.276 3(19)	−0.078 5(10)	0.605 3(16)
O(4)	−0.044 4(23)	0.045 6(9)	−0.091 3(19)	C(27)	0.377 6(19)	−0.051 6(10)	0.667 4(16)
C(5)	0.002 3(31)	0.183 4(13)	−0.050 5(27)	C(28)	0.379 6(19)	−0.001 5(10)	0.655 7(16)
O(5)	−0.030 0(25)	0.212 6(11)	−0.114 9(21)	C(29)	0.288 6(19)	0.062 8(9)	0.015 0(15)
C(6)	0.399 2(36)	0.144 7(14)	0.308 5(29)	C(30)	0.246 9(19)	0.018 8(9)	0.036 8(15)
O(6)	0.490 8(27)	0.162 3(11)	0.361 9(23)	C(31)	0.266 8(19)	−0.024 0(9)	−0.005 7(15)
C(7)	0.290 7(31)	0.051 4(13)	0.259 1(26)	C(32)	0.328 3(19)	−0.022 8(9)	−0.070 1(15)
O(7)	0.313 3(26)	0.012 1(11)	0.284 6(21)	C(33)	0.370 0(19)	0.021 3(9)	−0.092 0(15)
C(8)	0.242 2(29)	0.240 0(12)	0.146 1(24)	C(34)	0.350 1(19)	0.064 1(9)	−0.049 4(15)
O(8)	0.288 9(27)	0.268 6(11)	0.113 1(23)	C(35)	0.349 4(17)	0.162 7(9)	0.034 8(17)
C(9)	−0.006 5(33)	0.245 5(13)	0.140 5(26)	C(36)	0.298 6(17)	0.187 1(9)	−0.056 6(17)
O(9)	−0.095 8(30)	0.265 3(11)	0.125 1(24)	C(37)	0.372 7(17)	0.216 3(9)	−0.088 1(17)
C(10)	0.201 9(33)	0.224 2(13)	0.321 2(29)	C(38)	0.497 7(17)	0.221 1(9)	−0.028 2(17)
O(10)	0.241 5(24)	0.235 2(9)	0.405 3(21)	C(39)	0.548 5(17)	0.196 8(9)	0.063 2(17)
C(11)	0.176 2(20)	0.107 5(6)	0.620 6(16)	C(40)	0.474 4(17)	0.167 6(9)	0.094 7(17)
C(12)	0.145 0(20)	0.079 5(6)	0.687 0(16)				

of **2** beyond $2\theta = 40°$. Both structures were solved by direct methods, light atoms being located by subsequent Fourier difference syntheses. The Ir and P atoms in both **2** and **4**, and C and O atoms in **2**, were allowed to vibrate anisotropically. Absorption corrections were applied by the Walker and Stuart method.[28] The H atoms of the phenyl groups were added in calculated positions (C–H 1.08 Å) and refined 'riding' on their respective C atoms. The SHELX 76[29] package of crystallographic programs has been used in all calculations. Fractional atomic coordinates for **2** and **4** are reported in Tables 8 and 9.

Additional material available from the Cambridge Crystallographic Data Centre comprises H-atom coordinates, thermal parameters and remaining bond lengths and angles.

Acknowledgements

We thank A. J. Poë for helpful kinetic discussions, S. Nayor (MRC Toxicology Unit) for FAB mass spectral measurements, M. Martinelli (Cambridge) and F. Y. Fujiwara (Campinas) for ^{31}P NMR data, J. Lewis and B. F. G. Johnson (Cambridge) for their help and encouragement, Johnson Matthey for a generous loan of $IrCl_3$, Conselho Nacional de Desenvolvimento Científico e Tecnológico (CNPq), Brazil (F. S. L., M. D. V.), FAPESP, Brazil (M. D. V.) and Ministero dell'Universitá e della Ricerca Scientifica e Tecnologica (MURST), Italy (D. B., F. G.) for research grants.

References

1 P. Braunstein and J. Rose, *Gold Bull.*, 1985, **18**, 17.
2 I. D. Salter, *Adv. Organomet. Chem.*, 1989, **29**, 249.
3 K. P. Hall and D. M. P. Mingos, *Prog. Inorg. Chem.*, 1984, **32**, 237.
4 J. W. Lauher and K. Wald, *J. Am. Chem. Soc.*, 1981, **103**, 7648.
5 R. Hoffmann, *Angew. Chem., Int. Ed Engl.*, 1982, **21**, 711.
6 See, for example, T. M. G. Carneiro, D. Matt and P. Braunstein, *Coord. Chem. Rev.*, 1989, **96**, 49; T. J. Henly, R. J. Shapley and A. L. Rheingold, *J. Organomet. Chem.*, 1986, **310**, 55; R. Della Pergola, L. Garlaschelli, F. Demartin, M. Manassero, N. Masciocchi and M. Sansoni, *J. Chem. Soc., Dalton Trans.*, 1990, 127; M. L. Blohm and W. L. Gladfelter, *Inorg. Chem.*, 1987, **26**, 459; A. Albinati, F. Demartin, P. Janser, L. F. Rhodes and L. M. Venanzi, *J. Am. Chem. Soc.*, 1989, **111**, 2115; S. B. Colbran, C. M. Hay, B. F. G. Johnson, F. Lahoz, J. Lewis and P. R. Raithby, *J. Chem. Soc., Chem. Commun.*, 1986, 1766; M. I. Bruce, P. E. Corbin, P. A. Humphrey, G. A. Koutsantonis, M. J. Liddell and E. R. T. Tiekink, *J. Chem. Soc., Chem. Commun.*, 1990, 674.
7 C. P. Horwitz and D. F. Shriver, *J. Am. Chem. Soc.*, 1985, **107**, 8147.
8 B. F. G. Johnson, D. A. Kaner, J. Lewis and M. J. Rosales, *J. Organomet. Chem.*, 1982, **238**, C73.
9 A. K. Chipperfield, C. E. Housecroft and A. L. Rheingold, *Organometallics*, 1990, **9**, 681.
10 C. E. Housecroft, M. S. Shongwe and A. L. Rheingold, *Organometallics*, 1989, **8**, 2651.
11 G. A. Carriedo, V. Riera, M. L. Rodriguez, P. G. Jones and J. Lautner, *J. Chem. Soc., Dalton Trans.*, 1989, 639.
12 J. N. Nicholls, P. R. Raithby and M. D. Vargas, *J. Chem. Soc., Chem. Commun.*, 1986, 1617.
13 B. E. Mann, R. Khattar and M. D. Vargas, unpublished work.
14 P. R. Raithby, M. D. Vargas and F. S. Livotto, unpublished work.
15 D. Braga, F. Grepioni, F. S. Livotto and M. D. Vargas, *J. Organomet. Chem.*, 1990, **391**, C28.
16 R. Ros, A. Scrivanti, V. G. Albano, D. Braga and L. Garlaschelli, *J. Chem. Soc., Dalton Trans.*, 1986, 2411.
17 See, for example, D. Braga and F. Grepioni, *J. Organomet. Chem.*, 1987, **336**, C9; A. Strawczynski, R. Ros, R. Roulet, D. Braga, C. Gradella and F. Grepioni, *Inorg. Chim. Acta*, 1990, **170**, 17.
18 L. Kane-Maguire, E. Sinn and M. D. Vargas, unpublished work.
19 V. Albano, P. Bellon and V. Scatturin, *Chem. Commun.*, 1967, 730.
20 S. Naylor and M. D. Vargas, *J. Organomet. Chem.*, 1990, **386**, 275.
21 D. C. Sonnenberger and J. D. Atwood, *J. Am. Chem. Soc.*, 1982, **104**, 2113.
22 D. J. Taube and P. C. Ford, *Organometallics*, 1986, **5**, 99.
23 A. J. Poë, in *Metal Clusters*, ed. M. Moskovits, Wiley, New York, 1986.
24 J. Powell, E. Fuchs, M. R. Gregg, J. Phillips and M. V. R. Steiner, *Organometallics*, 1990, **9**, 387.
25 S. B. Colbran, B. F. G. Johnson, J. Lewis and R. M. Sorrell, *J. Organomet. Chem.*, 1985, **296**, C1.
26 R. J. Whiman, *J. Chem. Soc., Dalton Trans.*, 1982, 2294.
27 C. G. Swain, M. S. Swain and L. F. Berg, *J. Chem. Inf. Comput. Sci.*, 1980, **20**, 47.
28 N. Walker and D. Stuart, *Acta Crystallogr., Sect. A*, 1983, **39**, 158.
29 G. M. Sheldrick, SHELX 76 system of computer programs, University of Cambridge, 1976.

Received 25*th June* 1991; *Paper* 1/03153H